



Published in final edited form as:

*J Cell Physiol.* 2013 January ; 228(1): 50–57. doi:10.1002/jcp.24102.

## Cytoskeletal remodeling of connective tissue fibroblasts in response to static stretch is dependent on matrix material properties

Rosalyn D Abbott<sup>1</sup>, Cathryn Koptiuch<sup>2</sup>, James C Iatridis<sup>3</sup>, Alan K Howe<sup>4</sup>, Gary J Badger<sup>5</sup>, and Helene M Langevin<sup>2,6,\*</sup>

<sup>1</sup>School of Engineering, University of Vermont, Burlington, VT

<sup>2</sup>Department of Neurology, University of Vermont, Burlington, VT

<sup>3</sup>Department of Orthopaedics, Mount Sinai School of Medicine, New York, NY

<sup>4</sup>Department of Pharmacology, University of Vermont, Burlington, VT

<sup>5</sup>Department of Medical Biostatistics, University of Vermont, Burlington VT

<sup>6</sup>Department of Orthopedics & Rehabilitation, University of Vermont, Burlington VT

### Abstract

In areolar “loose” connective tissue, fibroblasts remodel their cytoskeleton within minutes in response to static stretch resulting in increased cell body cross-sectional area that relaxes the tissue to a lower state of resting tension. It remains unknown whether the loosely arranged collagen matrix, characteristic of areolar connective tissue, is required for this cytoskeletal response to occur. The purpose of this study was to evaluate cytoskeletal remodeling of fibroblasts in and dissociated from areolar and dense connective tissue in response to 2 hours of static stretch in both native tissue and collagen gels of varying crosslinking. Rheometric testing indicated that the areolar connective tissue had a lower dynamic modulus and was more viscous than the dense connective tissue. In response to stretch, cells within the more compliant areolar connective tissue adopted a large “sheet-like” morphology that was in contrast to the smaller dendritic morphology in the dense connective tissue. By adjusting the *in vitro* collagen crosslinking, and the resulting dynamic modulus, it was demonstrated that cells dissociated from dense connective tissue are capable of responding when seeded into a compliant matrix, while cells dissociated from areolar connective tissue can lose their ability to respond when their matrix becomes stiffer. This set of experiments indicated stretch-induced fibroblast expansion was dependent on the distinct matrix material properties of areolar connective tissues as opposed to the cells’ tissue of origin. These results also suggest that disease and pathological processes with increased crosslinks, such as diabetes and fibrosis, could impair fibroblast responsiveness in connective tissues.

### Keywords

Fibroblasts; cytoskeleton; dense connective tissue; areolar connective tissue; mechanotransduction

\*Helene M Langevin, 89 Beaumont Ave, Burlington, VT 05405, USA, Telephone number: 802-656-1001, Fax number:802-656-8704, helene.langevin@uvm.edu.

The authors have no conflict of interests to declare.

The contents of this article are solely the responsibility of the authors and do not necessarily represent the official views of the National Center for Complementary and Alternative Medicine, National Institutes of Health.

## Introduction

Research on connective tissue to date has almost exclusively focused on specialized load bearing connective tissues (e.g. tendons, ligaments, joint capsules) rather than the ubiquitous “non-specialized” connective tissue. This connective tissue forms a network of fasciae surrounding and separating muscles and organs throughout the body. Non-specialized connective tissue is characterized by an irregularly woven pattern of collagen fibers that ranges from densely-packed to loosely-arranged (Imayama and Braverman, 1988; Kawamata *et al.*, 2003; McCombe *et al.*, 2001). Loose connective tissue, also known as “areolar”, differs from other connective tissues in that its role is not primarily load-bearing. Rather, areolar connective tissue layers act as compliant interfaces that allow adjacent dense connective tissue layers to move past one another (Langevin *et al.*, 2011b).

It was previously shown that, in areolar connective tissue, fibroblasts actively remodel their cytoskeleton within minutes in response to changes in tissue length (Langevin *et al.*, 2005). When areolar connective tissue is elongated either *ex vivo* or *in vivo*, fibroblasts actively spread out and remodel their cytoskeleton to form new lamellipodia, resulting in a measurable increase in cell body cross-sectional area (Langevin *et al.*, 2005). Importantly, this dynamic fibroblast spreading actively contributes to relaxing the tissue when it is elongated *ex vivo* (Langevin *et al.*, 2011a). It remains unknown whether the loosely arranged collagen matrix, characteristic of areolar connective tissue, is required for fibroblast-mediated tension regulation to occur. In denser connective tissues, fibroblasts may be shielded from tissue loads by the stiffer more organized collagen matrix and thus, might not exhibit cytoskeletal remodeling in response to tissue stretch.

The purpose of this study was to evaluate cytoskeletal remodeling of fibroblasts in and derived from the mouse areolar and dense connective tissue in response to stretch in both native tissue and collagen gels of varying crosslinking. We hypothesized that 1) dense connective tissue has a greater dynamic modulus than areolar connective tissue, 2) in dense connective tissue, fibroblasts do not increase their cross-sectional area in response to tissue stretch, 3) fibroblasts originating from dense connective tissue have an increased response to stretch when seeded into collagen gels with dynamic moduli equivalent to that of areolar connective tissue, 4) fibroblasts originating from areolar connective tissue have a decreased responsiveness to stretch when seeded into gels with dynamic moduli equivalent to that of dense connective tissue, and 5) morphological responses to stretch are reversible.

## Materials and Methods

Five complementary sets of experiments were completed: 1) *ex vivo* experiments to evaluate whether magnitude of tissue stretch influences fibroblast morphology within the areolar and dense connective tissue layers, 2) rheometric testing of areolar and dense connective tissues, as well as collagen gels of varying crosslinking, 3) *in vitro* experiments of fibroblasts dissociated from dense connective tissue and seeded in collagen gels with a modulus similar to areolar connective tissue, 4) *in vitro* experiments of fibroblasts dissociated from areolar connective tissue and seeded in collagen gels with different degrees of crosslinking to evaluate whether the modulus of the extracellular matrix affects the cellular response to stretch, and 5) *in vitro* experiments to determine if the morphological response to stretch is dynamic and reversible on a short time scale. The primary outcome measures were cell morphology (measured as cell body cross-sectional area) and dynamic modulus (determined by a rheometer).

### Tissue dissection, cell isolation, and collagen gel culture

Mice were sacrificed via decapitation with approval from the Animal Care and Use Committee. Subcutaneous connective tissue was harvested immediately after death from the back of C57Black6 male mice weighing 19–21g. For tissue stretch experiments *ex vivo*, a 2.5 × 3.5cm flap containing dermis, subcutaneous muscle, and subcutaneous tissue was dissected from the back wall musculature and excised (Figure 1A).

To obtain cells for seeding in collagen gels, tissue was excised in the same manner and areolar and dense connective tissues were dissected away from the surrounding subcutaneous tissues and enzymatically digested to release the cells (0.2% protease, 0.2% collagenase for a minimum of four hours, Sigma–Aldrich, St. Louis, MO). Isolated cells were washed once with phosphate buffered saline (PBS) containing 1.5% fungizone (Invitrogen Lifesciences- Gibco, Carlsbad, CA) and 3% penicillin/streptomycin (Gibco), and were expanded in high glucose DMEM (Gibco) containing 10% FBS (Gibco), 1% penicillin/streptomycin, 0.5% fungizone, and 50  $\mu\text{g/L}$  ascorbic acid (Sigma-Aldrich). Passage II cells were used for all studies.

Ribose glycation of collagen gels was used to test whether differences in matrix properties are responsible for decreased cytoskeletal remodeling in response to stretch. Exploiting ribose glycation to crosslink a collagen gel increases its tensile and compressive modulus (Girton *et al.*, 1999; Roy *et al.*, 2008), as well as increases the density of the matrix (Hwang *et al.*, 2011). Adding ribose while the collagen is still in solution (preglycation) vs. adding it in the media after gelation both result in the same increase in compressive modulus, however, adding the ribose in solution prior to cell seeding preserves cell viability (Roy *et al.*, 2008). Preglycated collagen gel solutions were created by combining Type I collagen (BD Biosciences, Product number 354249, San Diego, CA) and D-(–)-Ribose (Sigma Aldrich, Product number R9629) to a concentration of 250 mM prior to gelation (Roy *et al.*, 2008) and incubated at 5°C for 6 or 12 days. Cells derived from either the areolar or dense connective tissue were counted with a hemocytometer and suspended in one of three collagen solutions at a density of  $0.5 \times 10^6$  cells/mL: Unglycated, 6 days preglycated, or 12 days preglycated collagen each diluted with 0.1 normal NaOH, 10X DMEM, and FBS, to a final concentration of 3.1 mg/mL (pH of 7.4). 800  $\mu\text{L}$  was pipetted into a mold 2 cm × 2 cm to create a height of 0.2 cm for each gel. After 30 minutes the gels were released from the bottom of the mold to float for three days in basal media which was defined as high glucose DMEM with the addition of: 15mM HEPES (Gibco), 1% penicillin/streptomycin, 0.05% fungizone, 50  $\mu\text{g/L}$  ascorbic acid, and 1% Insulin-Transferrin-Selenium-G (Gibco). The average contraction over culture condition of the gels was 2.9 mm (SD of 1.0), 1.9 mm (SD of 0.6), and 1.6 mm (SD of 0.8) for unglycated, 6 days preglycated, and 12 days preglycated, respectively. The gels were then either mechanically tested on a rheometer, stained with a live/dead kit and imaged, or either stretched or floated for two hours.

### Rheometric testing

A 5 mm biopsy punch was used to punch cylindrical constructs out of the connective tissue and gels for testing with a rheometer (TA Instruments, New Castle, DE). Dynamic stiffness tests were carried out as described previously (Schek *et al.*, 2011) using flat platens covered with 100 grit sand paper and a humidified chamber. The test protocol consisted of a 20 minute equilibration at 0.1N of axial compression, followed by a dynamic frequency sweep at 10% strain from 0.032 to 32 Hz, finishing with a strain sweep at 0.5Hz from 1 to 500% strain. Dynamic modulus magnitude,  $|G^*|$ , and phase angle,  $\delta$ , were calculated at each point of the frequency and strain sweeps. Parameters from both frequency and strain sweeps demonstrated power law dependence for the connective tissue and collagen gels, and were fit with a least squares routine in Matlab as described previously (Schek *et al.*, 2011)

(Mathworks Inc., Natick, MA, USA, Supplement 1 for representative fits and chi square goodness of fit parameters). Eight parameters from the model fit were used to compare  $|G^*|$  and  $\delta$  across the groups.

Frequency Sweep:

$$|G^*|(\omega) = a + b\omega^{\alpha_{|G^*|}}$$

$$\delta(\omega) = c + d\omega^{\alpha_{\delta}}$$

Strain Sweep:

$$|G^*|(\gamma) = j + k(\gamma + \Gamma)^{\beta_{|G^*|}}$$

$$\Delta(\gamma) = m + n\gamma^{\beta_{\delta}}$$

For the frequency sweep, the magnitude of the dynamic modulus was characterized by its value at 1 Hz,  $|G^*|_{1\text{Hz}}$ , and its dependence on frequency was characterized by its power law exponent,  $\alpha_{|G^*|}$ . Strain rate viscosity effects (change in  $\delta$  with increasing frequency) were characterized by the magnitude of  $\delta$  at 1 Hz,  $\delta_{1\text{Hz}}$ , and its frequency dependence exponent,  $\alpha_{\delta}$ . Accurate fitting of the strain sweep modulus data required a strain offset term. The dynamic modulus during the strain sweep was characterized by the modulus at 1% strain,  $|G^*|_{1\%}$ , and strain dependence exponent,  $\beta_{|G^*|}$ . Phase angle magnitude was characterized by its value at 1% strain,  $\delta_{1\%}$ , and strain dependence exponent,  $\beta_{\delta}$ .

### Tissue and collagen gel stretching

Excised tissue flaps were placed between stainless steel grips as previously described (Langevin *et al.*, 2005) and immersed in HEPES physiological saline solution, pH 7.4 at 37°C, containing (mM): NaCl 141.8, KCl 4.7, MgSO<sub>4</sub> 1.7, EDTA 0.39, CaCl<sub>2</sub> 2.8, HEPES 10.0, KH<sub>2</sub>PO<sub>4</sub> 1.2, Glucose 5.0. Initial length between grips was 25mm for each tissue experiment. The zero load point was tissue placed in grips and incubated for 2 hours without elongation. Likewise, the gels were placed in rubber grips that were 12 mm apart, with each gel taut but not stretched (Figure 1B). The grips were then immersed in a bath containing the defined basal media. Unstretched gels were incubated in the same bath for 2 hours (Figure 1C).

The proximal grip for all experiments was connected to a 500-g (4.9 N)-capacity load cell. The gel or tissue was elongated by advancing a micrometer connected to the distal grip (~rate of 1 mm/s) until the targeted load was achieved and then maintained at that length for 2 hours. For the tissue experiments, the load varied between 0 and 170mN to determine the morphometric response at different forces, while for the gel experiments, the load was always at 20 mN. To examine the reversibility of the cellular response, one set of gel experiments also had an additional 10 minute release (by shortening the distance between the grips) after the 2 hour stretch. At the end of each incubation the whole tissue and gels were immersion fixed in 4% paraformaldehyde (PFA) in PBS, for 2 hours or 30 minutes, respectively, to obtain morphometric measurements.

### Immunohistochemistry

After fixation, areolar and dense subcutaneous connective tissue samples (5mm in width, 5mm in length) were dissected from the dermis and subcutaneous muscle. Five samples each of areolar and dense connective tissue were taken in succession. Beta-tubulin staining was used for morphometric measurements of the dense and areolar connective tissue, while phalloidin staining of cells in collagen gels was performed for morphometric measurements. The dense connective tissue was more impenetrable to staining, therefore it was determined that the phalloidin staining was not as accurate as  $\beta$ -tubulin staining. A separate set of experiments in areolar connective tissue verified that phalloidin and  $\beta$ -tubulin staining resulted in the same morphometric measurements (data not shown).

The fixed tissue and collagen gel samples were rinsed with PBS containing 1% Triton- 100  $\times$  for 30 minutes. Tissue samples were then incubated with a mouse monoclonal anti- $\beta$ -tubulin primary antibody (Sigma) at 1:100 dilution overnight at room temperature. They were washed three times in PBS containing 1% bovine serum albumin for 15 minutes, incubated in Alexa 488-conjugated goat anti-mouse antiserum (Invitrogen) at 1:100 dilution for 1 h at room temperature, and counterstained for 5 minutes with DAPI nucleic acid stain 1:6000 (Molecular Probes, Eugene OR). Fixed collagen gels were stained for polymerized actin using Texas redconjugated phalloidin 1:25 (4 U/ml; Molecular Probes, Eugene OR) for 1 hour at room temperature and counterstained for 10 minutes with DAPI nucleic acid stain 1:6000. Samples were mounted on slides with mountant media (Ted Pella, Product number 19470, Redding, CA).

### Imaging and morphometric measurements

Histochemically stained tissue and gel samples were imaged with a Zeiss LSM 510 META confocal scanning laser microscope. The tissue samples were imaged at 63x (oil immersion lens, N.A. 1.4) with four fields per sample, totaling 16 images per tissue type per experiment. The collagen gels were imaged at a smaller magnification (40x, oil immersion lens, N.A. 1.3) to fit more cells in a field since the cells were larger. At least four fields per sample were taken totally a minimal of 20 cells per experiment. For each field, a stack of approximately 25 images were acquired at a 0.53  $\mu$ m inter-image interval. The size of the stacks was determined by maximizing the number of cells. Stacks of individual images were used for morphometric analysis. Stacks were also made into projections. For all morphometric analyses, the experimental unit was considered one excised tissue flap or 4 cm<sup>2</sup> gel, in which the observation represented the mean of all cell measurements made across multiple images. Cell body cross-sectional area was evaluated as described previously (Langevin *et al.*, 2005), where a cell cytoplasm's was traced by following each one through successive optical sections within an image stack excluding cell processes which were defined as an extension of a cell's cytoplasm longer than 2  $\mu$ m and less than 2  $\mu$ m in width at any portion of its length (Figure 2).

### Cell viability

As cell viability had already been performed for the tissue *ex vivo* experiments (Langevin *et al.*, 2011a) it was only performed for the different gel conditions in the present study using the same Live/Dead kit (Invitrogen) and protocol Calcein (excitation 494nm/ emission 517nm) stains the cytoplasm of live cells green and Ethidium (excitation 528nm/ emission 617nm) stains the DNA of dead cells red. The gels were incubated in a 2 $\mu$ M Calcein AM/ 4 $\mu$ M Ethidium Homodimer-2 solution, for 15 minutes and imaged on an Olympus BX50 Light Microscope with a 20X objective (at least 5 images were taken per gel). The total number of live and dead cells were counted using ImageJ (National Institutes of Health, Bethesda, MD) and a viability percentage [Live Cells/Total Cells  $\times$  100] was calculated for each image.

## Statistical Methods

Within-animal morphometric comparisons of areolar and dense connective tissue at 20 mN of applied force were performed using a paired t-test. In addition, the relationship between force and cell cross-sectional area across a wide range of applied forces (0–170 mN) and its dependency on tissue type was examined using linear regression. A two-sample t-test was used to compare areolar vs. dense connective tissue taken from different animals on dynamic moduli. Comparisons of dynamic moduli outcomes and live/dead cell counts across gel conditions were performed using one way analyses of variance. A two-way analysis of variance was performed to compare morphometric measurements across stretch and gel conditions. The two fixed factors were stretch condition (stretch vs. no stretch) and gel condition (unglycated, preglycated 6 days with ribose, and preglycated 12 days with ribose). When appropriate, Fisher's Least Significant Difference (LSD) procedure was used to perform pairwise comparisons among experimental conditions. Lastly, comparisons between experimental conditions on cross-sectional area from the release experiment (no stretch vs. stretched 2 hours and released 10 minutes) were performed using a two-sample t-test. This set of experiments was limited to the unglycated gel condition. Analyses were performed using SAS (SAS Institute, Cary, NC) and Minitab (Minitab Inc, State College, PA) statistical software. Statistical significance was determined based on  $p < .05$ .

## Results

In response to static tissue stretch for 2 hours, cells within the areolar connective tissue adopted a larger "sheet-like" morphology. In contrast, cells within dense connective tissue had a similar appearance in stretched tissue compared with tissue incubated for 2 hours without stretch (Figure 3 A–D). With 20mN of applied force, cell body cross-sectional area was significantly greater in areolar compared with dense connective tissue ( $n=7$ , paired t-test,  $p < .001$ ). The difference in cellular response between dense and areolar connective tissue also was consistently observed over a wide range of applied forces from 0 to 170mN. Regression analyses indicated that cell cross-sectional area was significantly greater in areolar compared to dense connective tissue ( $F_{1,40}=5.2$ ,  $p < .05$ ) (Figure 3E). Furthermore, the relationship between force and cell cross-sectional area was dependent on tissue type ( $F_{1,40}=6.1$ ,  $p < .05$ ). Cell cross-sectional area significantly increased as a function of force in areolar ( $\beta=1.4$ ,  $F_{1,40}=4.4$ ,  $p < .05$ ), but not in dense connective tissue ( $\beta=-0.38$ ,  $F_{1,40}=2.3$ ,  $p=.20$ ). Therefore the ability of fibroblasts to remodel their cytoskeleton in response to stretch appears to be tissue-type specific (i.e. occurs in areolar but not dense connective tissue).

To investigate whether differences in cellular responses between the two tissue types is related to differences in tissue mechanical properties, we performed dynamic rheological testing of separate layers of dense and areolar connective tissue. Dense connective tissue had a higher dynamic modulus than areolar connective tissue demonstrated by both the strain sweep and frequency sweep curves (Figure 4,  $n=6$ , t-tests  $p < .001$  and  $p=.003$  respectively). The magnitude of the phase angle curve was higher for the areolar connective tissue ( $n=6$ , t-test, strain sweep,  $p=.022$ ), indicating that the areolar connective tissue is more viscous than the dense connective tissue. Areolar connective tissue also had a higher exponent to the frequency sweep curve ( $\alpha_{1G^*}$ ) than the dense connective tissue ( $n=6$ , t-test,  $p=.003$ ) indicating greater strain rate dependent stiffening. This indicates that fibroblasts within the two tissues are exposed to very different mechanical environments, the dense connective tissue being stiffer and less viscous than the areolar connective tissue.

In order to conduct experiments in which the cell source (i.e. areolar vs. dense connective tissue) and the matrix material properties are controlled separately, fibroblasts were dissociated from tissues and embedded into gels with varying amounts of crosslinking

induced by ribose glycation. The glycated and unglycated gels were tested to determine if they mimicked the material properties of the dense and areolar connective tissues respectively. Gels preglycated for 12 days had a higher dynamic modulus than both the unglycated gels and gels preglycated for 6 days ( $n=6$ , overall ANOVA F-test  $p=.029$  and  $p=.002$  for strain sweep and frequency, respectively, Fisher's LSD  $p<.05$ ). The preglycated 12 days gel was on the same order of magnitude as the dense connective tissue, while the unglycated and 6 days preglycated gels had a similar modulus to areolar connective tissue.

When fibroblasts dissociated from the areolar connective tissue were seeded into unglycated gels (similar stiffness to areolar connective tissue), they responded to stretch with a "sheetlike" morphology (Figure 5D) which was similar to their behavior in the native tissue (Figure 3D). Fibroblasts dissociated from dense connective tissue likewise became "sheet-like" when stretched in unglycated gels (Figure 5B), which was in contrast to their lack of response in their native stiffer tissue (Figure 3B). To quantify the difference in morphology between experimental conditions, cell body cross-sectional area was measured in stacks of confocal microscopy images. Fibroblasts from dense connective tissue seeded in unglycated gels had a significantly greater cross-sectional area in stretched compared with no-stretch conditions (Figure 6A,  $n=6$ , t-test,  $p = .006$ ). The areolar derived fibroblasts seeded into both unglycated and preglycated 6 days gels (similar modulus to areolar connective tissue), had a significantly higher cross-sectional area with stretch compared with no-stretch (Figure 6C,  $n=6$ , Two-way ANOVA F-test for gel by stretch interaction,  $p<.001$  and Fisher's LSD,  $p<.05$ ). In contrast, when fibroblasts derived from areolar connective tissue were seeded into preglycated 12 days gels (similar stiffness to dense connective tissue) there were no significant differences between the no stretch and stretch conditions (Figure 6B). Therefore, by controlling and varying the gel conditions, it was shown that 1) fibroblasts from dense connective tissue are capable of responding in a compliant matrix and 2) cells from areolar connective tissue can lose their ability to respond when their matrix environment becomes stiffer.

To determine if stretch-induced changes in cell morphology are dynamic and reversible, areolar derived fibroblasts were stretched in unglycated gels for 2 hours and then released for 10 minutes. After removing the mechanical stimulus for 10 minutes there were no significant differences between the unstretched and stretched cells in cell cross-sectional area ( $n=3$ , t-test,  $n=3$ ,  $p=.263$ ) (Figure 7). Although there was a trend toward decreased cell viability in the 12 days preglycated group, there were no significant differences in the viability percentage between gel conditions (Supplement 2,  $n=3$ , ANOVA F-test,  $p=.051$ ).

## Discussion

This study quantified the morphological response of fibroblasts in and dissociated from areolar and dense connective tissue in response to two hours of static stretch. Taken together this set of experiments showed that the stretch-induced change in fibroblast morphology was dependent on extrinsic matrix material properties as opposed to the cells' tissue of origin (Figure 8). In experiments involving *ex vivo* static stretching of whole tissue explants, fibroblasts within the areolar connective tissue adopted a larger "sheet-like" morphology that was in contrast to the smaller dendritic morphology in the dense connective tissue. By adjusting the *in vitro* collagen properties it was demonstrated that fibroblasts dissociated from dense connective tissue and seeded into a compliant matrix were capable of responding to static stretch. On the other hand, fibroblasts dissociated from areolar connective tissue and seeded into a stiffer environment lost their ability to respond to tissue stretch, suggesting effects were dominated by the matrix and not the cell. Changes in cytoskeletal remodeling were found to be dynamic, and were reversed after the mechanical stimulus was removed for ten minutes.

Because the areolar connective tissue was more compliant and viscous than the dense connective tissue our results suggest that a loosely arranged, compliant matrix is required for the fibroblasts to actively spread out and remodel their cytoskeleton in response to stretch. Interestingly, fibroblasts in 6 day preglycated gels had an intermediate response to stretch (less than the unglycated but more than 12 day preglycated gels) which may be due to the 6 day gels being denser and more organized (Hwang *et al.*, 2011) even though their modulus was not different from the unglycated gels. Our results also suggest that, in highly crosslinked 12 day gels, fibroblasts may have been further shielded from tissue loads by the stiffer and more organized collagen matrix, or were adapting to the stiffer environment, as smaller cells are exposed to smaller principal stresses and strains than larger cells of the same shape (Gupta and Haut Donahue, 2006).

Our results suggest that, *in vivo*, the response of areolar connective tissue fibroblasts to static tissue stretch may become impaired in the presence of pathologies that increase matrix density via collagen crosslinking. In particular our *in vitro* model used non-enzymatic glycation crosslinking, which results in advanced glycation end products (AGEs) that are associated with diabetes and aging (Bruehl and Oxlund, 1996; Reiser, 1991; Singh *et al.*, 2001; Verzijl *et al.*, 2000; Vlassara and Striker, 2011; Wang *et al.*, 2002). A potential limitation of using ribose for inducing glycation *in vitro* is that ribose can increase cell death when it is in the culture media (Han *et al.*, 2011; Roy *et al.*, 2008). However, in our experiments the gels were preglycated which has been shown to preserve cell viability (Roy *et al.*, 2008). In this study there was a trend toward decreased cell viability in the 12 days preglycated cells, but it was a minor effect that was not statistically significant. We cannot rule out, on the other hand, that the presence of residual AGEs could have had other effects depending on tissue type and culture system including stimulation of pro-inflammatory cytokines (Singh *et al.*, 2001). Inflammation could in addition modulate the transition into a myofibroblast phenotype (Hinz, 2009), although, this was not the subject of this study since myofibroblast transformation is a longer term phenotypic adaptation that occurs over days, whereas the cytoskeletal responses that we examined were rapid and reversible as previously demonstrated in whole tissue *ex vivo* (Langevin *et al.*, 2005; Langevin *et al.*, 2010).

Our results also may have implications for our understanding of connective tissue pathology associated with chronic pain. This includes patients with low back pain that have increased thickness and echogenicity of the connective tissues forming the thoracolumbar fascia and impaired mobility between the areolar and dense layers (Langevin *et al.*, 2011b; Langevin *et al.*, 2009). Our current results suggest that cells in the denser connective tissues may not have the capacity to adjust resting tension as dynamically as in less dense connective tissue (Langevin *et al.*, 2011a).

In conclusion, fibroblasts in both dense connective tissue and stiff crosslinked gels did not exhibit cytoskeletal remodeling in response to tissue stretch. However, a loosely arranged compliant collagen matrix, characteristic of areolar connective tissue, promoted fibroblast cytoskeletal remodeling in response to stretch regardless of the fibroblast's tissue of origin (Figure 8). These results suggest that there are distinct roles of fibroblasts within areolar and dense connective tissues that are dependent on their mechanical environment, with fibroblasts having diminished mechanical responsiveness in the dense tissues. Morphological changes in response to stretch were found to be reversible on a short time scale, suggesting this is a dynamic process that is used to modulate mechanical properties of the areolar, and not dense, connective tissue.

## Supplementary Material

Refer to Web version on PubMed Central for supplementary material.

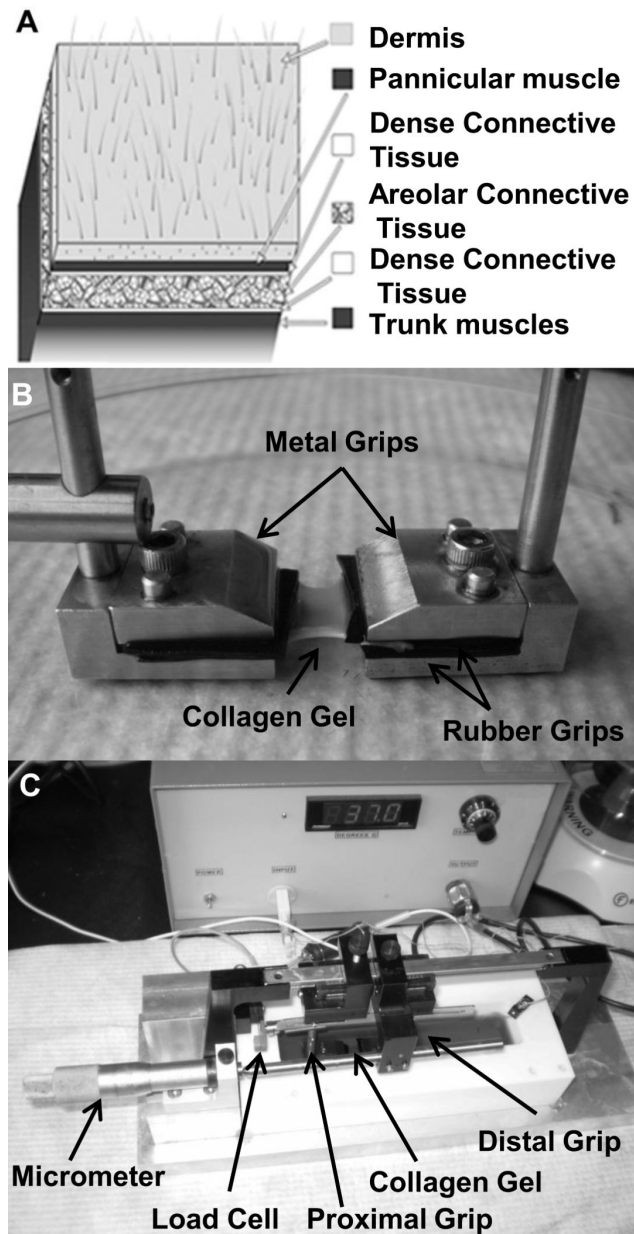
## Acknowledgments

This work was funded in part by the National Center of Complementary Medicine (R01AT001121) and by NIAMS (R01AR051146 & R01 AR057397) of the NIH.

## References

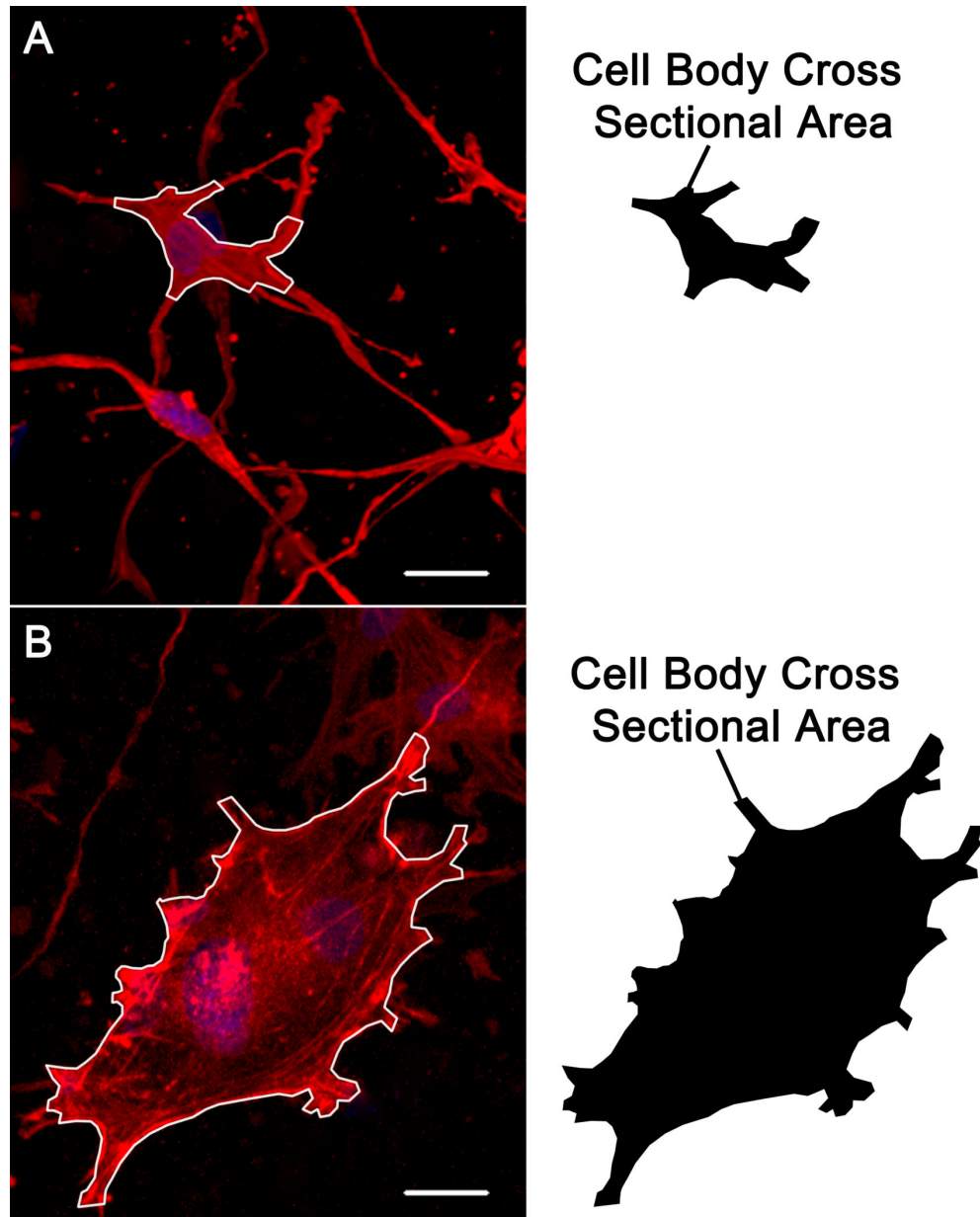
- Bruel A, Oxlund H. Changes in biomechanical properties, composition of collagen and elastin, and advanced glycation endproducts of the rat aorta in relation to age. *Atherosclerosis*. 1996; 127(2): 155–165. [PubMed: 9125305]
- Girton TS, Oegema TR, Tranquillo RT. Exploiting glycation to stiffen and strengthen tissue equivalents for tissue engineering. *J Biomed Mater Res*. 1999; 46(1):87–92. [PubMed: 10357139]
- Gupta T, Haut Donahue TL. Role of cell location and morphology in the mechanical environment around meniscal cells. *Acta Biomater*. 2006; 2(5):483–492. [PubMed: 16860617]
- Han C, Lu Y, Wei Y, Liu Y, He R. D-ribose induces cellular protein glycation and impairs mouse spatial cognition. *PLoS One*. 2011; 6(9):e24623. [PubMed: 21966363]
- Hinz B. Tissue stiffness, latent TGF-beta1 activation, and mechanical signal transduction: implications for the pathogenesis and treatment of fibrosis. *Curr Rheumatol Rep*. 2009; 11(2):120–126. [PubMed: 19296884]
- Hwang YJ, Granelli J, Lyubovitsky JG. Multiphoton optical image guided spectroscopy method for characterization of collagen-based materials modified by glycation. *Anal Chem*. 2011; 83(1):200–206. [PubMed: 21141843]
- Imayama S, Braverman IM. Scanning electron microscope study of elastic fibers of the loose connective tissue (superficial fascia) in the rat. *Anat Rec*. 1988; 222(2):115–120. [PubMed: 3213961]
- Kawamata S, Ozawa J, Hashimoto M, Kurose T, Shinohara H. Structure of the rat subcutaneous connective tissue in relation to its sliding mechanism. *Arch Histol Cytol*. 2003; 66(3):273–279. [PubMed: 14527168]
- Langevin HM, Bouffard NA, Badger GJ, Iatridis JC, Howe AK. Dynamic fibroblast cytoskeletal response to subcutaneous tissue stretch ex vivo and in vivo. *Am J Physiol Cell Physiol*. 2005; 288(3):C747–C756. [PubMed: 15496476]
- Langevin HM, Bouffard NA, Fox JR, Palmer BM, Wu J, Iatridis JC, Barnes WD, Badger GJ, Howe AK. Fibroblast cytoskeletal remodeling contributes to connective tissue tension. *J Cell Physiol*. 2011a; 226(5):1166–1175. [PubMed: 20945345]
- Langevin HM, Fox JR, Koptiuch C, Badger GJ, Greenan-Naumann AC, Bouffard NA, Konofagou EE, Lee WN, Triano JJ, Henry SM. Reduced thoracolumbar fascia shear strain in human chronic low back pain. *BMC Musculoskelet Disord*. 2011b; 12:203. [PubMed: 21929806]
- Langevin HM, Stevens-Tuttle D, Fox JR, Badger GJ, Bouffard NA, Krag MH, Wu J, Henry SM. Ultrasound evidence of altered lumbar connective tissue structure in human subjects with chronic low back pain. *BMC Musculoskelet Disord*. 2009; 10:151. [PubMed: 19958536]
- Langevin HM, Storch KN, Snapp RR, Bouffard NA, Badger GJ, Howe AK, Taatjes DJ. Tissue stretch induces nuclear remodeling in connective tissue fibroblasts. *Histochem Cell Biol*. 2010; 133(4): 405–415. [PubMed: 20237796]
- McCombe D, Brown T, Slavin J, Morrison WA. The histochemical structure of the deep fascia and its structural response to surgery. *J Hand Surg Br*. 2001; 26(2):89–97. [PubMed: 11281657]
- Reiser KM. Nonenzymatic glycation of collagen in aging and diabetes. *Proc Soc Exp Biol Med*. 1991; 196(1):17–29. [PubMed: 1984239]
- Roy R, Boskey AL, Bonassar LJ. Non-enzymatic glycation of chondrocyte-seeded collagen gels for cartilage tissue engineering. *J Orthop Res*. 2008; 26(11):1434–1439. [PubMed: 18473383]
- Schek RM, Michalek AJ, Iatridis JC. Genipin-crosslinked fibrin hydrogels as a potential adhesive to augment intervertebral disc annulus repair. *Eur Cell Mater*. 2011; 21:373–383. [PubMed: 21503869]
- Singh R, Barden A, Mori T, Beilin L. Advanced glycation end-products: a review. *Diabetologia*. 2001; 44(2):129–146. [PubMed: 11270668]

- Verzijl N, DeGroot J, Oldehinkel E, Bank RA, Thorpe SR, Baynes JW, Bayliss MT, Bijlsma JW, Lafeber FP, Tekoppele JM. Age-related accumulation of Maillard reaction products in human articular cartilage collagen. *Biochem J.* 2000; 350(Pt 2):381–387. [PubMed: 10947951]
- Vlassara H, Striker GE. AGE restriction in diabetes mellitus: a paradigm shift. *Nat Rev Endocrinol.* 2011; 7(9):526–539. [PubMed: 21610689]
- Wang X, Shen X, Li X, Agrawal CM. Age-related changes in the collagen network and toughness of bone. *Bone.* 2002; 31(1):1–7. [PubMed: 12110404]

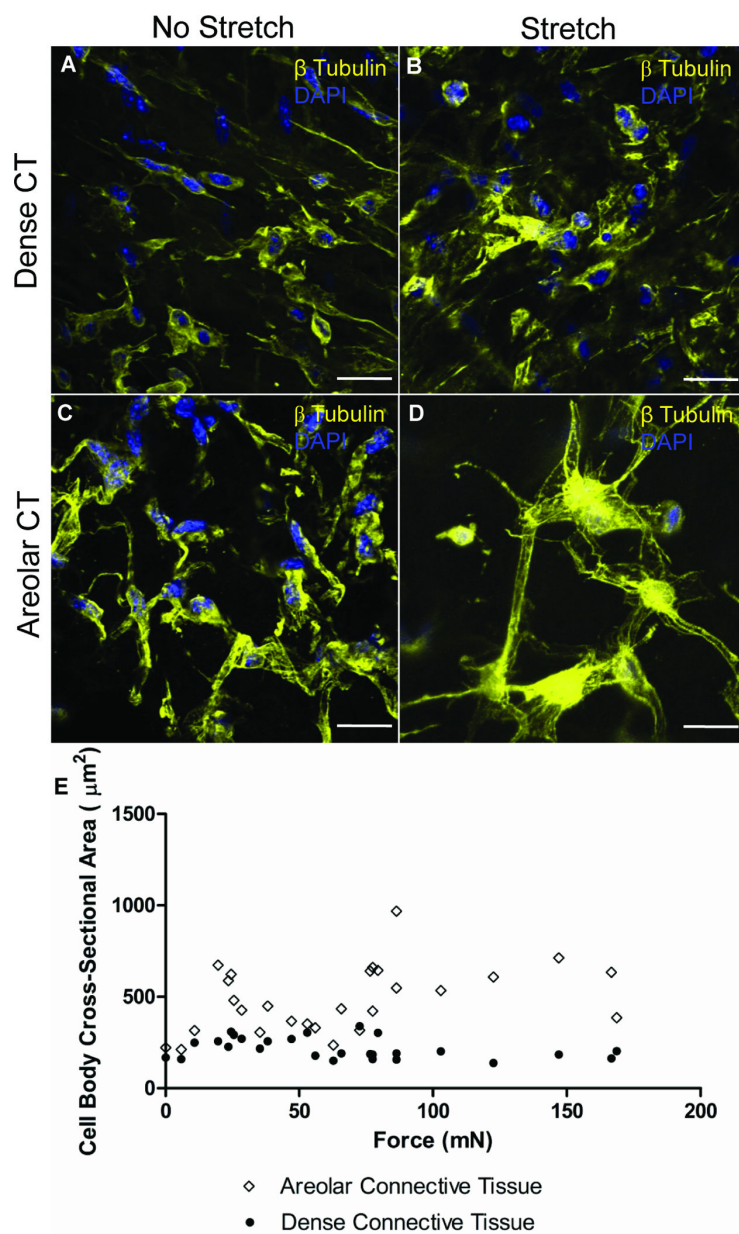


**Figure 1. Experimental Setup**

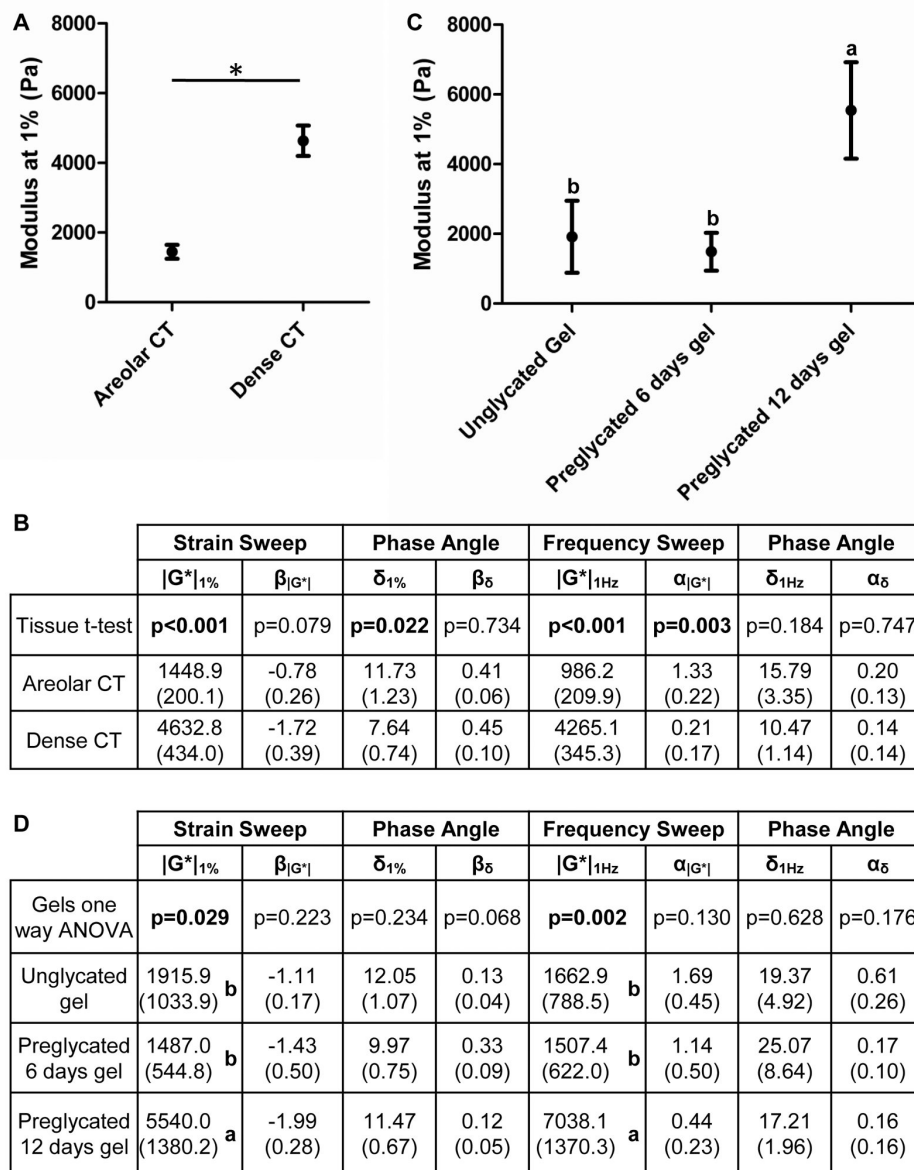
Schematic demonstrating different layers of mouse subcutaneous tissue that were dissected in this study (A). Collagen gel held between 2 rubber grips, and secured with outer metal grips (B). The grips mounted into the tissue stretching device (C).



**Figure 2. Experimental measurements of cell body cross-sectional area used to quantify different cell morphologies**  
Examples of morphometric measurements for “dendritic” (A) and “sheetlike” (B) cells (Bar=20  $\mu\text{m}$ , merged z-stack).

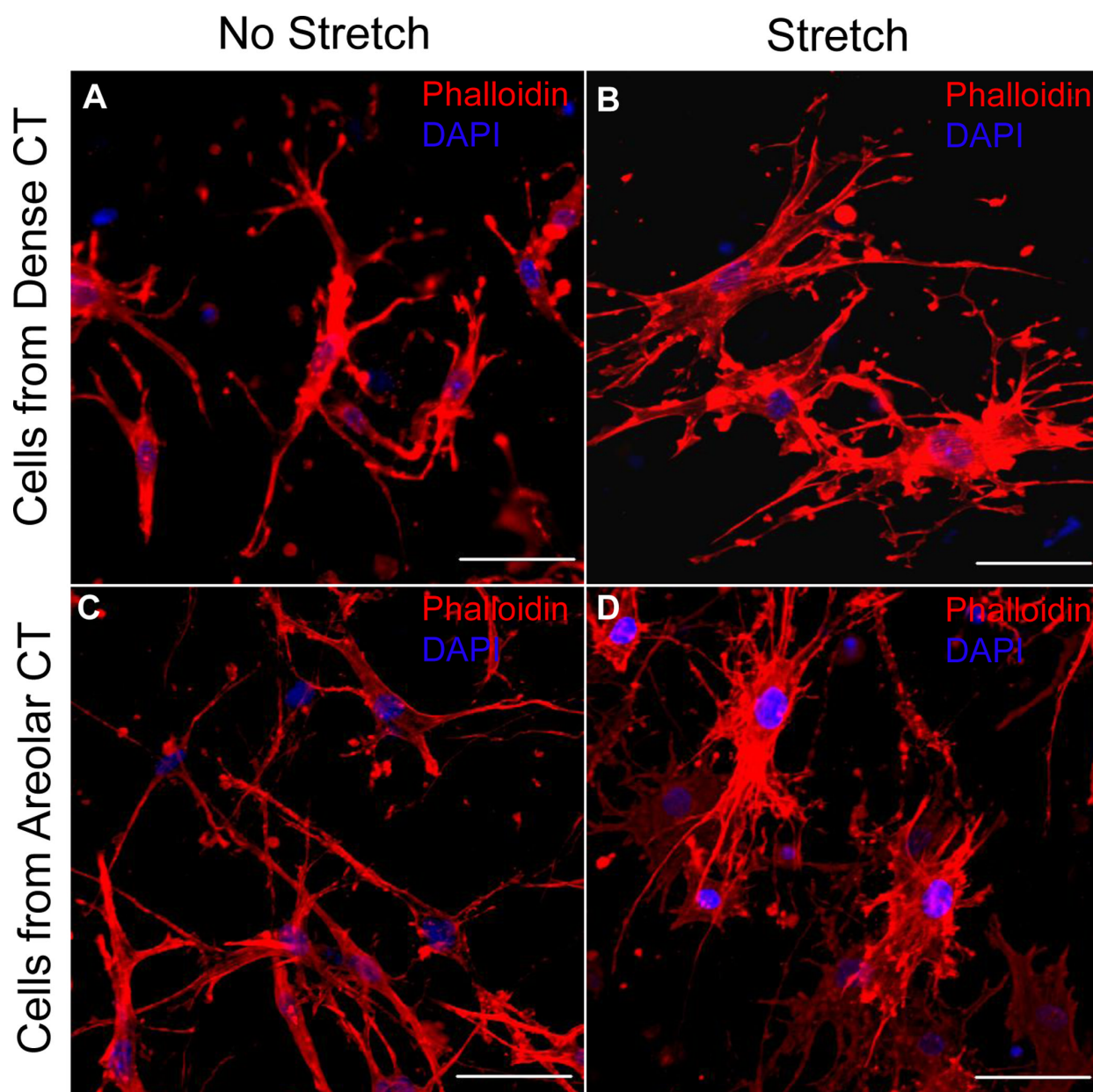


**Figure 3. Effect of static tissue stretch for 2 hours on dense and areolar connective tissue *ex vivo*** Morphology of fibroblasts within dense connective tissue unstretched (A) and stretched (B) compared to areolar connective tissue unstretched (C) and stretched (D). Cell cross-sectional area (E) was significantly increased as a function of force in areolar ( $\beta=1.4$ ,  $F_{1,40}=4.4$ ,  $p<.05$ ), but not in dense connective tissue ( $\beta=-0.38$ ,  $F_{1,40}=2.3$ ,  $p=.20$ ).

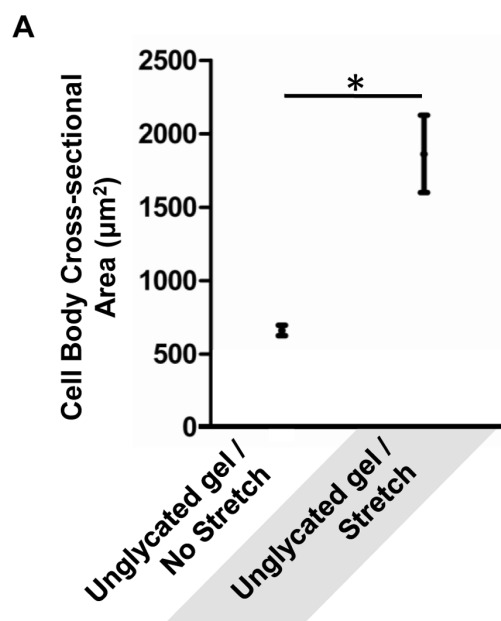
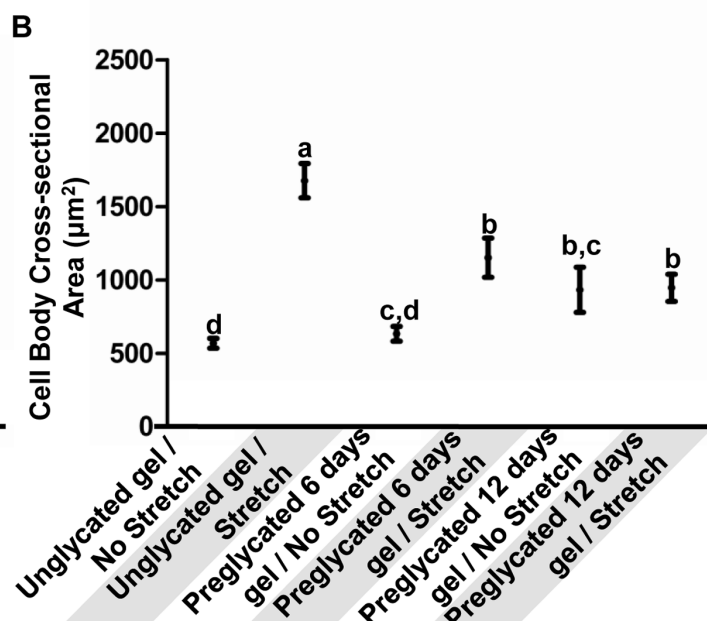


**Figure 4. Determination of connective tissue and collagen gel stiffness**

Dense connective tissue had a higher dynamic modulus than areolar connective tissue (A) demonstrated by both the strain sweep and frequency sweep curves (B) (n=6, t-test, p values shown for each parameter). The magnitude of the phase angle curve ( $\delta_{1\%}$ ) and the exponent to the frequency sweep curve ( $\alpha_{|G^*|}$ ) were significantly higher for the areolar connective tissue compared to the dense connective tissue. The preglycated 12 days gel had a higher dynamic modulus than the unglycated gel and preglycated 6 days gel (C) indicated by both the strain sweep and frequency sweep (D, n=6, one way ANOVA, strain sweep p values shown for each parameter, Fisher's LSD p<0.05). Gel groups sharing a common letter were not significantly different. Error bars represent SEM.



**Figure 5. Effect of static stretch for 2 hours on fibroblasts dissociated from dense and areolar connective tissue and seeded in unglycated collagen gels**  
 Cells from dense connective tissue (A,B) and cells from areolar connective tissue (C,D) were seeded into collagen gels having a similar stiffness to areolar connective tissue. The left images represent the no stretch condition (A,C) with images on the right representing the stretch condition (B,D). Cells derived from both tissue sources responded to stretch with an increase in cell cross sectional area (Phalloidin = red, Dapi = blue, bar=50  $\mu$ m, merged z-stack).

**Cells derived from Dense CT****Cells derived from Areolar CT**

**Figure 6. Morphological measurements of fibroblasts dissociated from dense and areolar connective tissue and seeded in collagen gels of varying crosslinking**

Fibroblasts dissociated from dense connective tissue were seeded into unglycated collagen gels (similar modulus to areolar connective tissue) and responded to stretch with an increase in cell body cross-sectional area (A)(n=6, t-test,  $p = .006$ ). Fibroblasts dissociated from areolar connective tissue were seeded into gels of different glycation durations corresponding to different stiffnesses (6 days had a similar modulus to areolar connective tissue while preglycated 12 days had a similar modulus to dense connective tissue) and cell body cross-sectional area was compared with and without static stretching of the gel. Interactions between the 6 groups demonstrated significant differences between stretch and no stretch for the unglycated and preglycated 6 days gels for cell cross-sectional area with no differences between the no stretch and stretch condition for the preglycated 12 days gels(interaction  $p < .001$ , Fisher's LSD,  $p < .05$ ). Gel groups sharing a common letter were not significantly different. Error bars represent SEM.

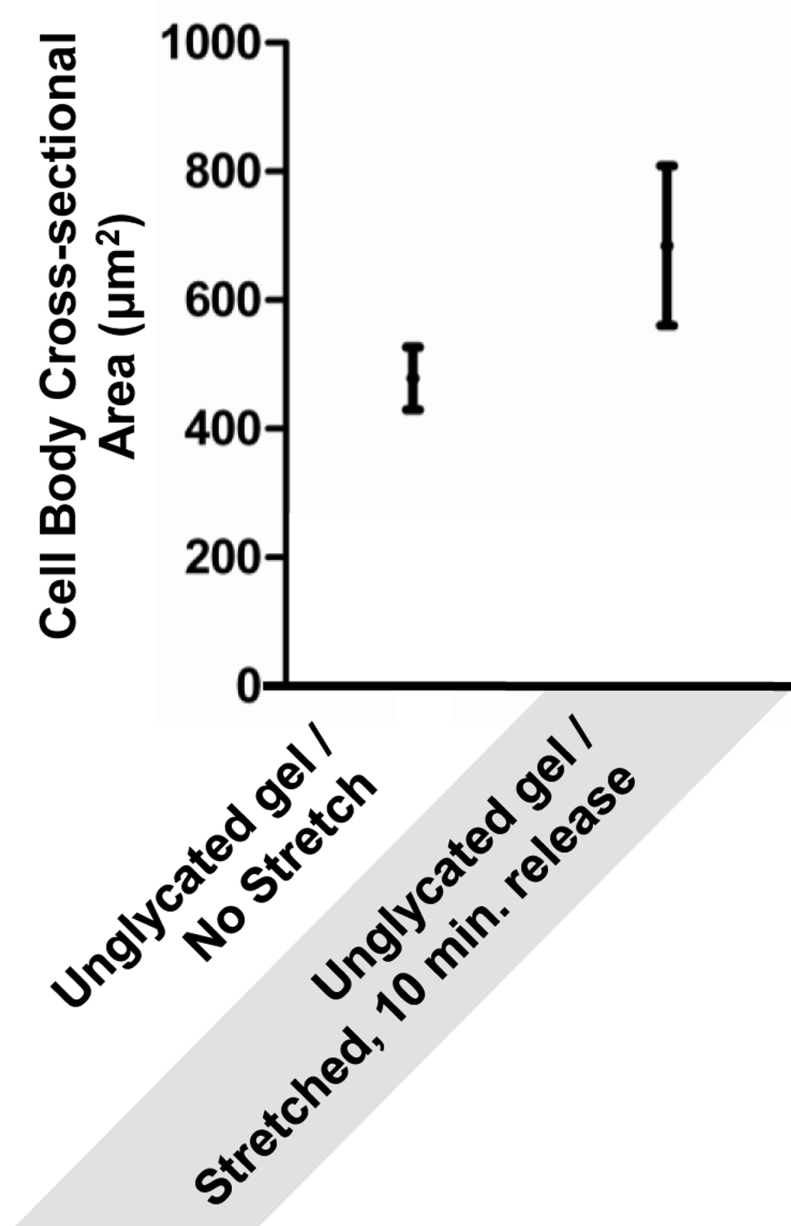


**Figure 7. Morphological effects are dynamic**

There are no significant differences in cell body cross-sectional area of fibroblasts stretched for 2 hours and then released for 10 minutes and fibroblasts that were not stretched ( $n=3$ ,  $t$ -test,  $p=.26$ ). Error bars represent SEM.

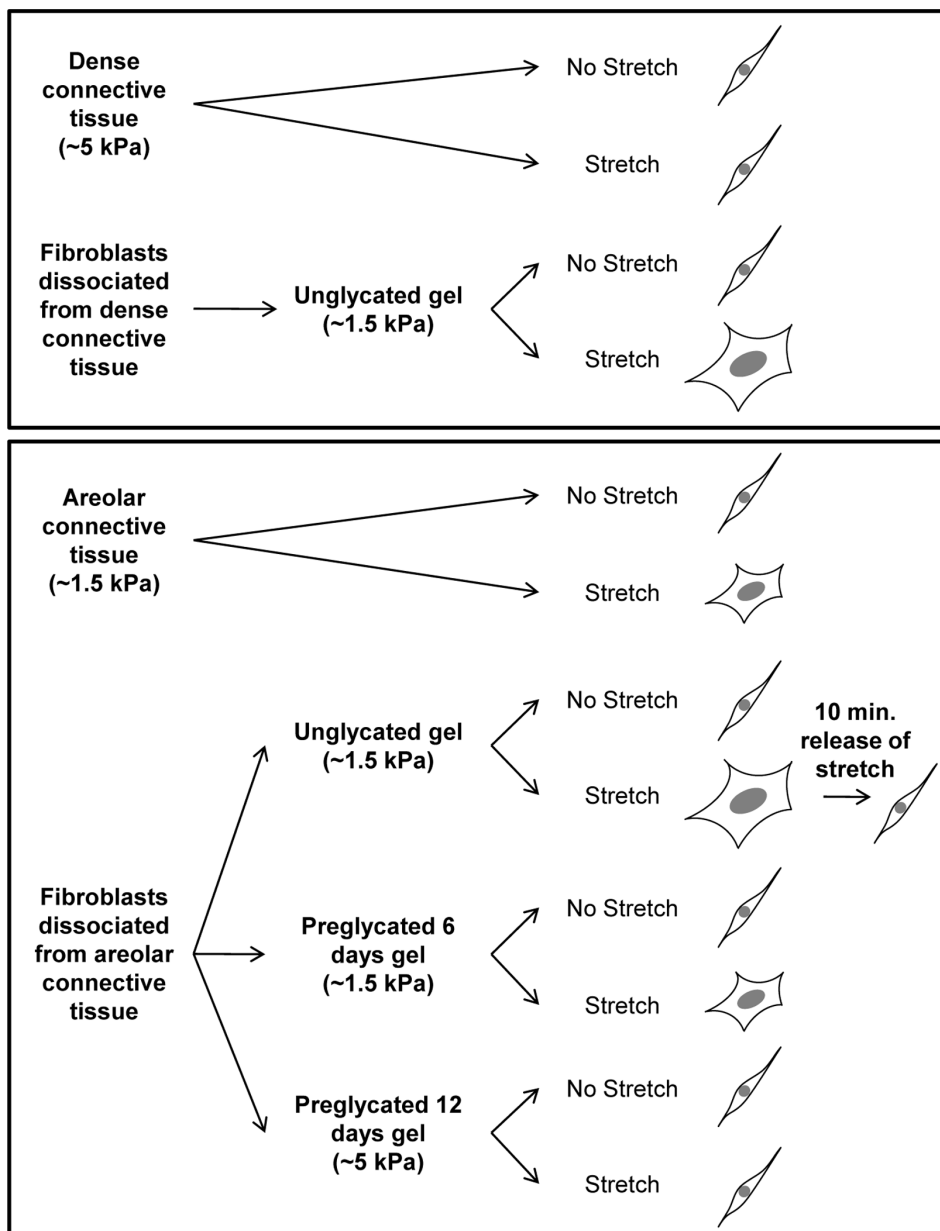


**Figure 8. Schematic representation of results**

Fibroblast expansion in response to stretch was only observed in tissue and gels (unglycated and 6 days preglycated) with a similar modulus to areolar connective tissue regardless of fibroblast tissue of origin.